Pharmaceutical Sciences and Drug Design
ISSN: 3062-4428
2023, Volume 3, Page No: 210-223

Available online at: www.galaxypub.co/page/journals

Galaxy Publication

Role of OmpH in Cec4-Mediated Reduction of Acinetobacter baumannii Biofilm

Ricardo Pinto[1]*, Andre Sousa[1]

[1]Department of Biotechnology, Faculty of Sciences, University of Coimbra, Coimbra, Portugal.

***E-mail** ✉ ricardo.pinto.pt@outlook.com

Received: 15 February 2023; **Revised:** 29 May 2023; **Accepted:** 01 June 2023

ABSTRACT

The rise of carbapenem-resistant Acinetobacter baumannii (CRAB) presents significant challenges in clinical management and has been identified by the World Health Organization as a priority pathogen requiring new antibiotic strategies. In our previous study, the novel antimicrobial peptide Cec4 demonstrated notable efficacy in reducing clinical CRAB biofilms, yet its underlying mechanism remains unclear. To assess the therapeutic potential of Cec4, it is essential to investigate how it disrupts mature biofilms.Transcriptomic analysis was employed to identify key genes associated with CRAB biofilm reduction by Cec4. Based on bioinformatic findings, the CRISPR-Cas9 system was used to generate gene deletion strains, and the pYMAb2 plasmid facilitated the creation of complementation strains. The involvement of these genes in Cec4-mediated biofilm disruption was then evaluated using crystal violet staining, podocyte staining, laser confocal microscopy, and determination of MBC and MBEC50 values.Transcriptome data suggested that OmpH is a critical gene in the Cec4-mediated removal of CRAB biofilms. While deletion of OmpH did not affect bacterial growth, it reduced capsule thickness, enhanced biofilm formation, and increased the susceptibility of biofilm-embedded A. baumannii to Cec4.Cec4 disrupts CRAB biofilms through targeting OmpH. Loss of OmpH leads to thicker biofilms but simultaneously increases bacterial sensitivity to Cec4, thereby facilitating more effective biofilm removal.

Keywords: OmpH, Acinetobacter baumannii, Antimicrobial peptide, Antibiofilm mechanism

How to Cite This Article: Pinto R, Sousa A. Role of OmpH in Cec4-Mediated reduction of Acinetobacter baumannii biofilm. Pharm Sci Drug Des. 2023;3:210-23. https://doi.org/10.51847/AFVSVjF1Kp

Introduction

Acinetobacter baumannii, a Gram-negative pathogen frequently encountered in intensive care units (ICUs) and operating rooms, represents a significant opportunistic threat in healthcare settings worldwide [1]. This bacterium rapidly acquires multidrug-resistant and even pan-resistant phenotypes at an alarming rate [2], contributing to approximately 60% of hospital-acquired infections. A. baumannii can cause a range of infections, including ventilator-associated pneumonia, bloodstream infections, and skin and soft tissue infections, affecting both healthy and immunocompromised individuals [3]. Unfortunately, the development of effective antibiotics against Gram-negative bacteria has lagged due to their diverse resistance mechanisms [4].

Biofilms are structured bacterial communities composed of extracellular polysaccharides, DNA, and secreted proteins [5], and they are a major driver of antibiotic resistance in A. baumannii, with most infections being biofilm-associated. Biofilm formation, from initial adhesion to mature development, involves complex regulation of multiple genes. For instance, the Csu operon, part of the fimbrial system, mediates adhesion, and its expression is regulated by quorum sensing pathways and two-component systems such as BfmS/R and GacSA. Additionally, genes encoding outer membrane proteins (OMPs) initiate biofilm formation, while phosphoglucose mutase (PGM) contributes to the biofilm matrix [6]. These genes are closely linked to the biofilm formation process in A. baumannii. Biofilms confer significant antibiotic resistance, resulting in mortality rates ranging from 40% to 60% [7]. For example, the A. baumannii ST1894 strain exhibits a 2048-fold increase in resistance to imipenem and a 32-fold increase to fucoxanthin when in a biofilm state [8]. The protective structure of biofilms enables

infections to persist for extended periods, spreading to other organs and becoming progressively resistant to antibiotics [9, 10]. Thus, biofilm-associated A. baumannii poses a greater clinical threat than planktonic cells, highlighting the importance of developing strategies to target biofilm-residing bacteria.

Antimicrobial peptides (AMPs) are key components of innate immunity in humans and other organisms and are currently a major focus of antimicrobial research [11]. These short polypeptides, typically fewer than 50 amino acids in length, are amphiphilic and carry a net positive charge [12, 13], allowing them to bind to negatively charged bacterial membranes, inhibit growth, and exert bactericidal effects. AMPs have been shown to inhibit or eliminate bacterial biofilms through several mechanisms [14], including disruption of cellular signaling [15], suppression of stress-response systems, inhibition of RNA synthesis [16], and downregulation of binding protein transporter genes essential for biofilm formation [17]. However, the detailed processes by which AMPs disrupt biofilms remain incompletely understood [18].

Cecropin-4 (Cec4), an AMP, demonstrates potent activity against Gram-negative bacteria, particularly A. baumannii [19, 20]. Preliminary studies have shown that Cec4 effectively reduces carbapenem-resistant A. baumannii biofilms [21]; however, the specific targets and mechanisms involved remain unclear. Building on our previous work, we employed transcriptomic and proteomic analyses to investigate the action of Cec4 on biofilms of carbapenem-resistant A. baumannii using high-throughput sequencing and tandem mass spectrometry. Based on these omics analyses, we performed gene knockout experiments to explore the regulatory mechanisms and potential molecular targets of Cec4 in biofilm clearance.

Materials and Methods

Strain culture conditions and Cec4

A. baumannii ATCC 17978 was maintained at the School of Biology and Engineering, Guizhou Medical University. Cec4 (GWLKKKIGKKKIERVGQNTRDATIQAIGVAQQQAANVAATLKGK) was synthesized to >97% purity using high-performance liquid chromatography (HPLC) via solid-phase chemical synthesis by Gill Biochemicals (Shanghai) Co. Ltd.

Bacterial stocks were stored at −80 °C. Glycerol stocks were removed and streaked onto plates using an inoculating loop. Following overnight incubation at 37 °C, single colonies were selected and cultured in 5 mL of Luria-Bertani (LB) broth at 37 °C with shaking at 220 rpm until reaching the logarithmic growth phase for subsequent phenotypic assays.

Transcriptome data analysis

Transcriptome sequencing data (PRJNA607078) were downloaded from the Sequence Read Archive (SRA) at the National Center for Biotechnology Information (NCBI) and subjected to quality control using fastp software (https://github.com/OpenGene/fastp) to remove low-quality reads and unknown bases, generating clean reads. Data analysis was conducted in R (https://cran.r-project.org/) and Bioconductor (https://www.bioconductor.org/) using the A. baumannii ATCC 19606 reference genome.

Bioinformatics analysis of OmpH

Due to limited reports on OmpH, bioinformatic analyses were performed. The protein sequence was analyzed with SignalP 5.0 for signal peptides, TMHMM for transmembrane domains, and SMART for domain architecture. Hydrophilicity was predicted using ProtScale. OmpH and Cec4 structures were modeled using Discovery Studio 2019 (DS2019) and AlphaFold2 [22], with molecular docking performed in DS2019.

Homologs of OmpH were identified in Escherichia coli [23], Bdellovibrio bacteriovorus [24], Flavobacterium psychrophilum [25], Pasteurella multocida [26], and Klebsiella spp. [27]. NCBI BLAST was used to identify sequences with 100% coverage and identity, followed by phylogenetic analysis using MEGA11 with the neighbor-joining method.

Construction of the OmpH mutant strain

The OmpH deletion strain was generated using CRISPR-Cas9 following Wang *et al*. [28]. Shuttle plasmids pCasAb and pSGAb, expressing Cas9, RecAb recombinase, and sgRNA, were used. Homologous repair ssDNA was synthesized by Sangon Biotech Co. Ltd. Recipient cells were prepared by washing with 10% sterile glycerol at 4 °C, and plasmids along with ssDNA were sequentially electroporated. Cas9 and RecAb expression were

induced with IPTG. Positive transformants were identified via resistance markers, and gene deletion was verified by colony PCR and sequencing.

ΔOmpH complementation strain construction

The OmpH gene was amplified using primers OmpH-F (5′→3′: CGCGGATCCTGGTCCAATTTGGTACAGAG) and OmpH-R (5′→3′: GCTCGAGTGCGGCCGCACTCGCCAAGTTTGAAAATT) and cloned into BamHI and NotI sites of pYMAb2-Hyg plasmid. The construct was introduced into the OmpH deletion strain via electroporation to generate the complemented strain ΔOmpH. The empty pYMAb2-Hyg plasmid served as the vector control. Successful complementation was confirmed by sequencing.

Determination of growth curve

Fresh bacterial suspensions were adjusted to 1×10^6 CFU/mL in TSB medium, and 200 μL of this suspension was added to each well of a 96-well plate, which was incubated continuously for 24 h. The optical density (OD) at intervals of 2 h was measured using the Agilent BioTek Cytation5 multifunction enzyme labeler to monitor bacterial growth.

Quantification of biofilm formation in A. baumannii

Biofilm production was quantified using crystal violet staining as previously described [29]. After removing the planktonic cells, the bacteria were washed, resuspended, and adjusted to 1 × 10^6 CFU/mL in TSB medium. Then, 200 μL of bacterial suspension was added to each well of a 96-well plate, with three replicates per group. The control group received TSB medium only. After incubation at 37 °C for 24 h, free bacteria were removed, and 200 μL of 10% methanol was added per well for 30 min to fix the biofilm. The biofilm was stained with 0.1% crystal violet solution, washed three times with PBS, and the OD_620 was measured after solubilizing the dye in 95% ethanol.

Gene expression analysis

Total RNA was extracted using the M5 EASY spin plus kit (Mei5 Biotechnology Co. Ltd), and complementary DNA (cDNA) was synthesized with the RR047A reverse transcription kit (Takara). RT-qPCR was performed in 10 μL reactions using ROX and 16S rRNA as internal controls. Expression levels of the most differentially expressed genes (H1126, H1233, H3691, CspG, GspG, and PaaH) and other biofilm-associated genes were analyzed before and after OmpH knockdown using the $2^{-\Delta\Delta CT}$ method.

Minimal Inhibitory Concentration (MIC) assay

MIC assays were performed as previously described [30]. Mueller-Hinton Broth (MHB) was added to each well of a 96-well plate (100 μL/well). Cec4 solution was added to achieve a final concentration of 128 μg/mL, and 100 μL from this solution was serially diluted across wells to obtain final concentrations of 1, 2, 4, 8, 16, and 32 μg/mL after addition of bacterial suspension at 2 × 10^6 CFU/mL. Negative and blank controls did not receive Cec4. Plates were incubated at 37 °C for 16–20 h, and MIC was defined according to CLSI standards as the lowest concentration preventing visible bacterial growth.

Broth and agar dilution methods

Using previously published methods with minor modifications [30], LB agar plates containing 1/2 MIC of Cec4 were prepared, and different concentrations of bacterial suspensions (1–10^6 CFU/mL) were spotted. Colony growth was assessed after 8 h.

Minimal Bactericidal Concentration (MBC) assay

TSB medium containing sequential concentrations of Cec4 (1/16×MIC to 8×MIC) was prepared, with three replicates per concentration, and incubated at 37 °C. Blank and negative control wells contained medium only or bacterial suspension only, respectively. The final bacterial concentration was adjusted to 1 × 10^7 CFU/mL as previously described [31]. Cec4 inhibition of biofilm formation before and after gene knockout was determined using crystal violet staining.

Minimal Biofilm Eradication Concentration (MBEC) assay

Bacterial suspensions at 1×10^6 CFU/mL were inoculated into 96-well plates (200 µL/well) [32]. Plates containing TSB medium without bacteria served as blank controls. Cec4 was added at final concentrations of 4–512 µg/mL, and plates were incubated at 37 °C for 24 h. Biofilm content was quantified by crystal violet staining, and the clearance rate was calculated as: clearance rate = (OD_620 experimental / OD_620 control) × 100%. MBEC_50 values were recorded for each group.

Capsule staining

Slides were prepared with 10 µL Congo red dye and 3 µL bacterial suspension (1 × 10^6 CFU/mL). After air-drying, slides were decolorized with 5% hydrochloric acid for 30 s, rinsed with ddH_2O, and stained with crystal violet for 1 min. Following rinsing and drying, slides were examined under a 100× inverted microscope (CKX53, Olympus) and photographed.

Statistical analysis

Bioinformatics figures and graphs were generated in R v4.2.1, while other images were prepared using GraphPad Prism 9. Two-group comparisons were performed using t-tests, and multiple-group comparisons were analyzed using one-way ANOVA.

Results and Discussion

Transcriptome of A. baumannii with strong biofilm phenotype after Cec4 treatment

To investigate the mechanism of Cec4-mediated biofilm removal, transcriptome data from A. baumannii with strong biofilm-forming ability following Cec4 treatment were reanalyzed using the ATCC 19606 genome. Initial sequencing data contained adapter and low-quality reads, which were removed during quality control. For example, single-end sequencing of ABF1 showed improved base quality after filtering, with no significant overall changes.

Principal component analysis (PCA) indicated that, despite outliers in Con2 and ABF4 samples, the between-group differences exceeded within-group differences, confirming the suitability of the data for downstream analyses.

Differential gene expression analysis using normalized counts and a coefficient of variation matrix identified 425 genes significantly affected by Cec4 treatment, including 242 upregulated and 183 downregulated genes (|log2FC| > 1, $P < 0.05$). A volcano plot illustrated these differentially expressed genes **(Figure 1a)**, while a heatmap of the top 20 genes by |log2FC| demonstrated consistent within-group expression, with most significantly altered genes being upregulated following Cec4 exposure **(Figure 1b).**

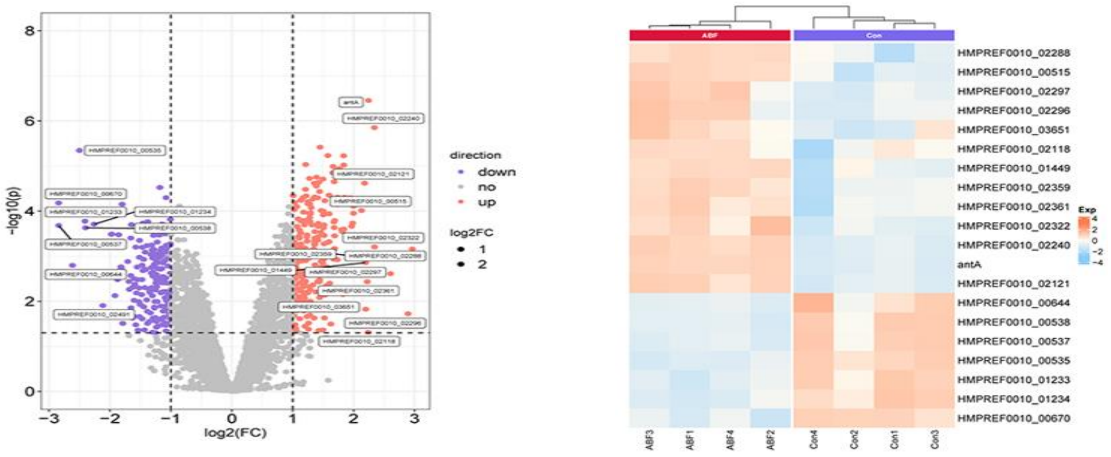

a) b)

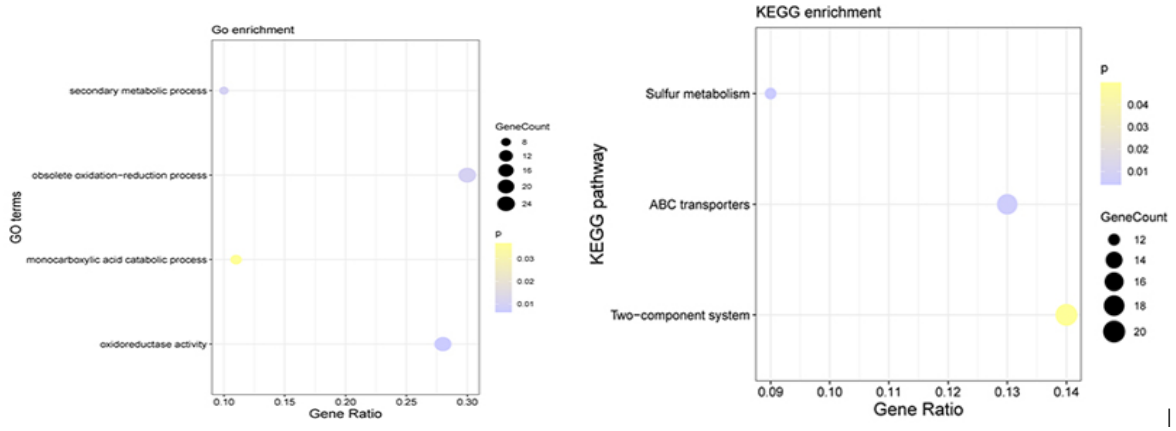

c) d)

Figure 1. Transcriptomic Analysis of A. baumannii with Strong Biofilm Treated by Cec4. (a) Volcano plot of differentially expressed genes, with genes meeting |log2FC| > 2 and P < 0.05 annotated. (b) Heatmap showing expression of the top 20 differentially expressed genes after normalization; colors indicate expression levels. Most genes exhibited consistent expression within groups, and those significantly altered by Cec4 treatment were primarily upregulated. (c) Bubble plot of GO enrichment for differentially expressed genes. (d) Bubble plot of KEGG enrichment for differentially expressed genes.

Gene Ontology (GO) and KEGG pathway enrichment

GO enrichment analysis of the differentially expressed genes revealed significant involvement in four biological pathways: secondary metabolic processes, redox reactions, monocarboxylic acid catabolism, and oxidoreductase activity **(Figure 1c).** KEGG pathway enrichment analysis identified significant involvement in sulfur metabolism, ABC transport, and two-component systems **(Figure 1d).**

RT-qPCR validation of transcriptome data

To confirm the transcriptomic findings, several genes showing differential expression were selected for reverse transcription quantitative PCR (RT-qPCR). The results demonstrated that HMPREF0010_02297 (H2297), PgaA, HMPREF0010_02766 (H2766), HMPREF0010_01126 (H1126), GspG, HMPREF0010_02313 (H2313), HMPREF0010_03691 (H3691), PaaH, CspG, and HMPREF0010_01233 (H1233) exhibited up- or downregulation patterns consistent with the transcriptomic analysis.

Identification of key genes during Cec4-mediated biofilm clearance

To refine candidate genes for knockout experiments, the thresholds for differential expression were tightened to padj < 0.05, yielding 338 differentially expressed genes, of which 208 were upregulated and 130 downregulated **(Figure 2a).** Sixteen genes were associated with the ABC transporter pathway **(Figure 2b)**, primarily encoding components of the binding protein-dependent transport system responsible for amino acid and sulfur/phosphate transport. Within this pathway, Glt-family genes were mostly downregulated, while Ssu-family genes were generally upregulated.

Antimicrobial peptides such as Cec4 may inhibit or disrupt biofilms by interfering with cell signaling, suppressing bacterial stress responses, downregulating binding protein transporter genes necessary for biofilm formation, and altering membrane potential within biofilms. Functional enrichment analysis of differentially expressed genes revealed significant GO terms including redox processes (BP) and oxidoreductase activity (MF), while KEGG enrichment highlighted the ABC transporter pathway **(Figures 3a and 3b)**. After narrowing the GO-enriched genes to 22 related to redox processes, these were not selected as candidates because redox-related proteins are broadly involved in bacterial physiology and unlikely to be specific targets of Cec4 in biofilm clearance. Nevertheless, the GO results indicated that Cec4 does interfere with redox processes in A. baumannii.

Based on this analysis, proteins associated with the ABC transporter pathway from KEGG enrichment and outer membrane-related proteins from differential gene annotation were selected as candidate genes for further investigation. Detailed information on these candidate genes is provided in **Table 1.**

Table 1. The candidate genes selected from the transcriptome

Gene	Protein	log_2FC	*P* value
KEGG-ABC transporter			
aotQ	–	1.479873143	0.000332958
glnQ	D0C804	−1.658356275	0.000395028
gltI	D0C807	−1.603455392	0.009493657
gltK	D0C805	−1.45762851	0.000184436
hisM	–	1.29203391	0.000113647
HMPREF0010_00886	–	1.189703016	0.001059408
HMPREF0010_01038	–	1.290063642	0.000108447
HMPREF0010_01713	–	1.153820896	0.003645927
HMPREF0010_02504	D0CCM4	1.515294175	0.000346461
HMPREF0010_02965	–	1.034329905	0.001250861
HMPREF0010_03358	–	1.46539906	0.001734293
HMPREF0010_03359	D0CF29	1.033785341	0.006549767
HMPREF0010_03362	–	1.095054779	0.000570843
metI	–	1.44042682	0.003325411
pstB	D0CBX9	−1.516288566	0.001054119
tauA	D0C855	1.105759376	0.007925973
Anno-Outer membrane			
HMPREF0010_00354	D0C6H4	−1.173563632	0.000844949
HMPREF0010_00477	D0C6U7	1.494831376	1.95E-05
HMPREF0010_00883	D0C803	1.675727823	0.000174084
HMPREF0010_01445	–	1.210494913	0.001251835
HMPREF0010_01710	–	−1.315163688	0.00056472
HMPREF0010_01714	D0CAD4	1.14440349	0.000746119
oprM	D0CDQ0	−1.061593702	0.003945246

Notes: "–" in the table denotes genes for which no corresponding proteins were identified in the transcriptome; KEGG-ABC transporter refers to genes significantly enriched in the ABC transporter pathway in KEGG; and Anno-Outer membrane indicates genes associated with the outer membrane according to differential gene annotation.

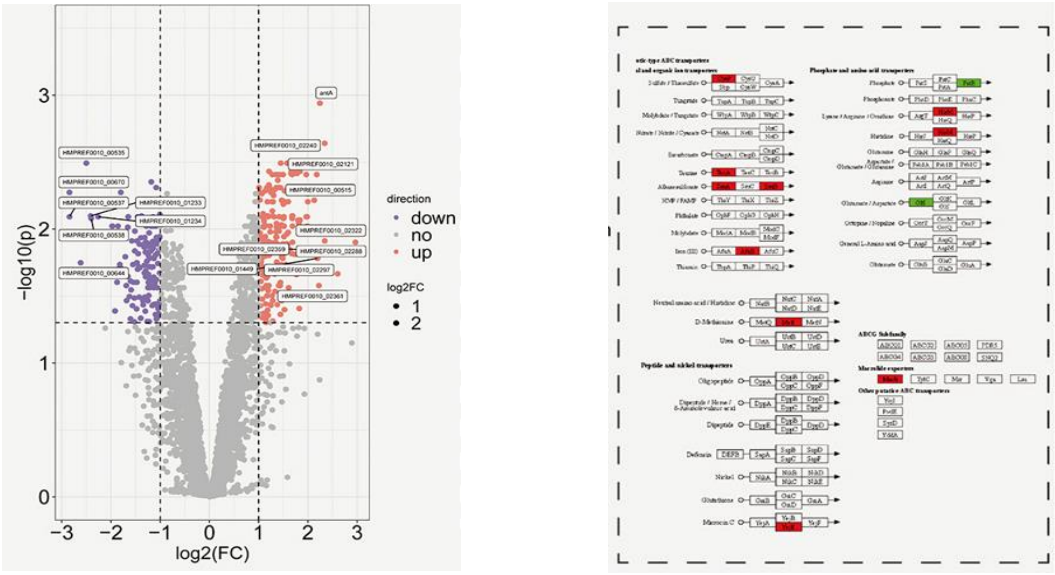

a) b)

Figure 2. Adjusted differential genes and ABC transporter pathway genes. (a) Volcano plot of differentially expressed genes after adjustment for padj. (b) Genes enriched in the ABC transporter pathway, identified through KEGG functional enrichment analysis of the adjusted differential genes from (b).

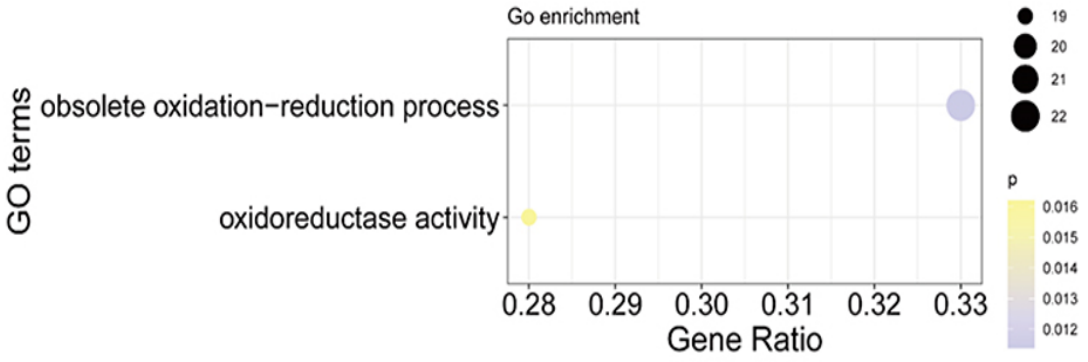

a)

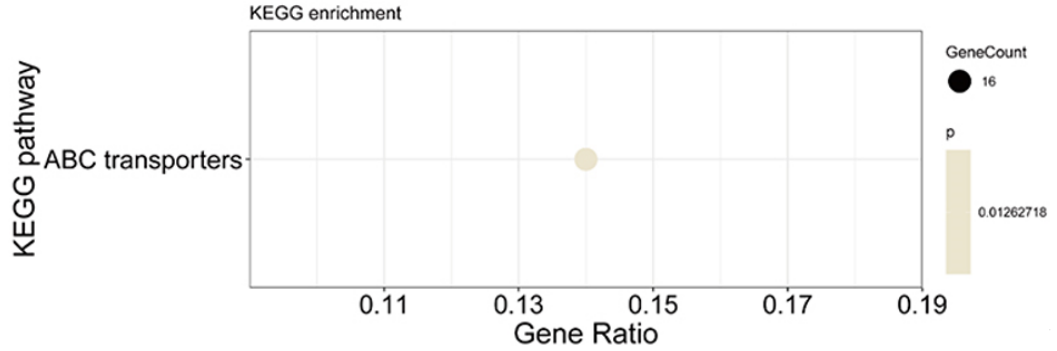

b)

Figure 3. GO and KEGG Enrichment Bubble Plots. (a) Adjusted GO pathways showing significant enrichment. (b) Adjusted KEGG pathways with significant enrichment.

Previous observations using laser confocal microscopy demonstrated that Cec4 localizes primarily on the outer membrane of A. baumannii. Guided by this finding, we focused on seven genes from the transcriptome associated with the outer membrane **(Table 1).** Of these, three were downregulated, and only HMPREF0010_00354 (OmpH) had a corresponding protein, making it a novel target for study in A. baumannii. Structural domain analysis confirmed that this protein contains an OmpH domain **(Figure 4a)**, and the generation of the OmpH knockout strain is shown in **Figure 4b.**

Bioinformatic predictions indicated that OmpH is 167 amino acids in length and may undergo N-terminal cleavage of a 23-residue signal peptide. The protein displays a hydrophobic N-terminal region and a hydrophilic C-terminal region, with a predicted molecular weight of 18,710.3 Da and a transmembrane segment, resembling OmpH-like proteins in Xanthomonas caldophilus. Three-dimensional models of both OmpH and Cec4 were constructed **(Figures 4c and 4d)**, and their interaction was examined through protein docking using DS2019 **(Figure 4e).** Phylogenetic analysis revealed low sequence similarity of OmpH between A. baumannii and other bacterial species **(Figure 4f).**

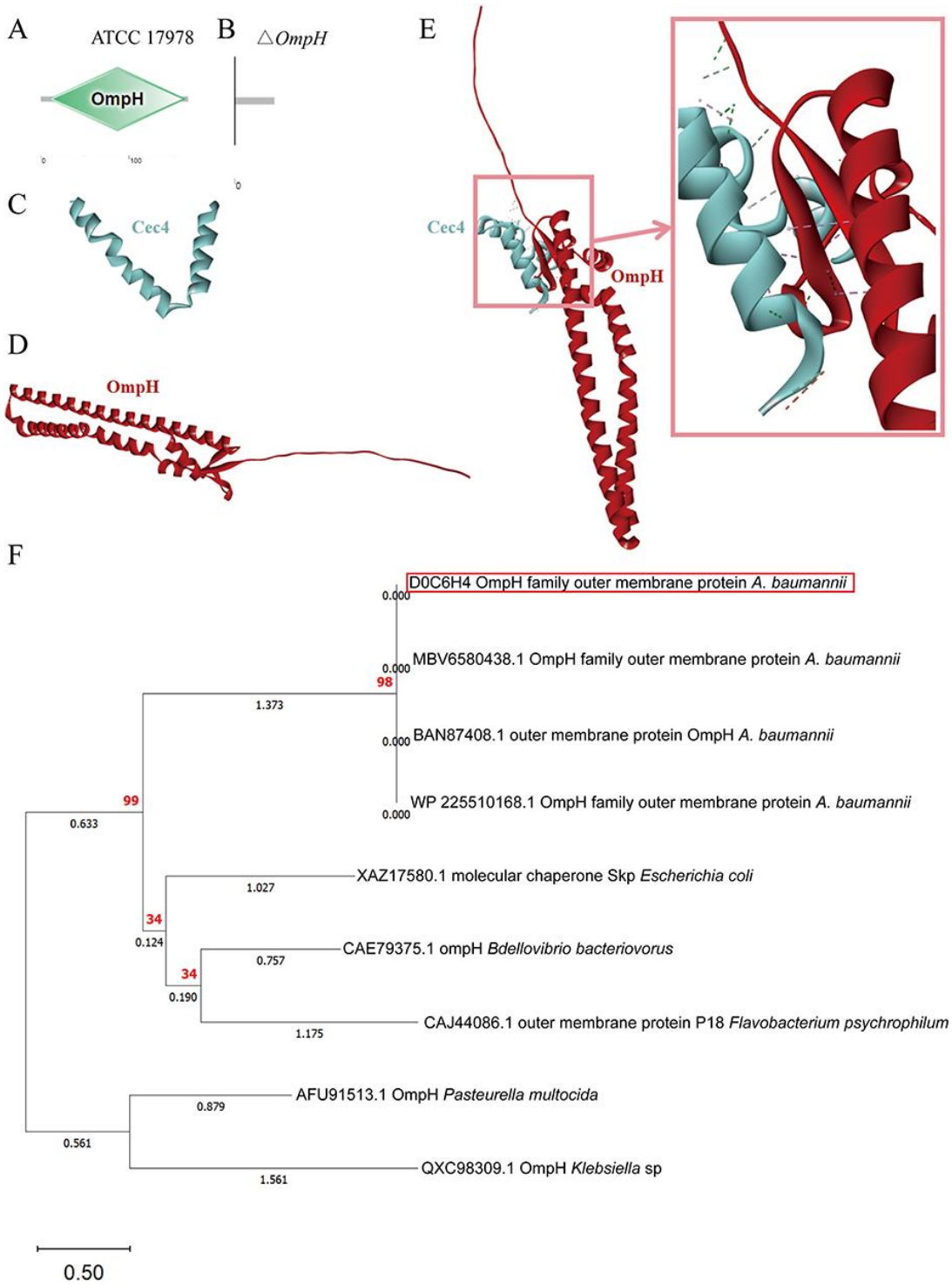

Figure 4. Bioinformatics predictions and molecular docking analyses of OmpH. (A) SMART-predicted structural domains of OmpH. (B) SMART-predicted structural domains for the OmpH deletion. (C) AlphaFold2-predicted 3D structure of Cec4. (D) AlphaFold2-predicted 3D structure of OmpH. (E) Protein–protein docking results between Cec4 and OmpH. (F) Phylogenetic tree analysis following OmpH BLAST; the red box highlights OmpH.

OmpH gene knockout

OmpH deletion strains were generated using the CRISPR-Cas9 system. A vector plasmid containing the full OmpH gene fragment was then constructed using the pYMAb2-Hyg expression plasmid for complementation. The CRISPR-Cas9 pSGAb plasmid carries a kanamycin-resistance marker; however, since the clinical strain CRAB78 is kanamycin-resistant, ATCC 17978 was selected for the deletion strain construction.

Effects of OmpH on A. baumannii growth and biofilm formation

We assessed growth **(Figure 5a)** and biofilm formation **(Figure 5b)** in the wild-type (ATCC 17978), OmpH-knockout (ΔOmpH), and back-complemented (ΔOmpH::OmpH) strains. Growth curves were similar among all strains during the first 4 h of incubation. From 4 to 8 h, ΔOmpH showed slightly reduced growth compared with ATCC 17978 and ΔOmpH::OmpH, but after 10 h, growth curves overlapped completely **(Figure 5a)**, indicating that OmpH deletion did not markedly affect overall growth. Notably, ΔOmpH produced significantly more biofilm than ATCC 17978 ($P < 0.05$) and a similar amount to ΔOmpH::OmpH **(Figure 5b).** Previous research has shown that OmpH acts as an upstream regulator of LuxR. Experiments in Vibrio alginolyticus demonstrated that OmpH's regulation of LuxR and biofilm formation is temperature-dependent; at 22°C, OmpH deletion upregulated LuxR and reduced biofilm, whereas at 37°C, the OmpH-deficient strain exhibited significantly higher biofilm than wild-type strains [33]. In this study, A. baumannii was cultured at 37°C, suggesting that the observed increase in biofilm formation may be linked to temperature.

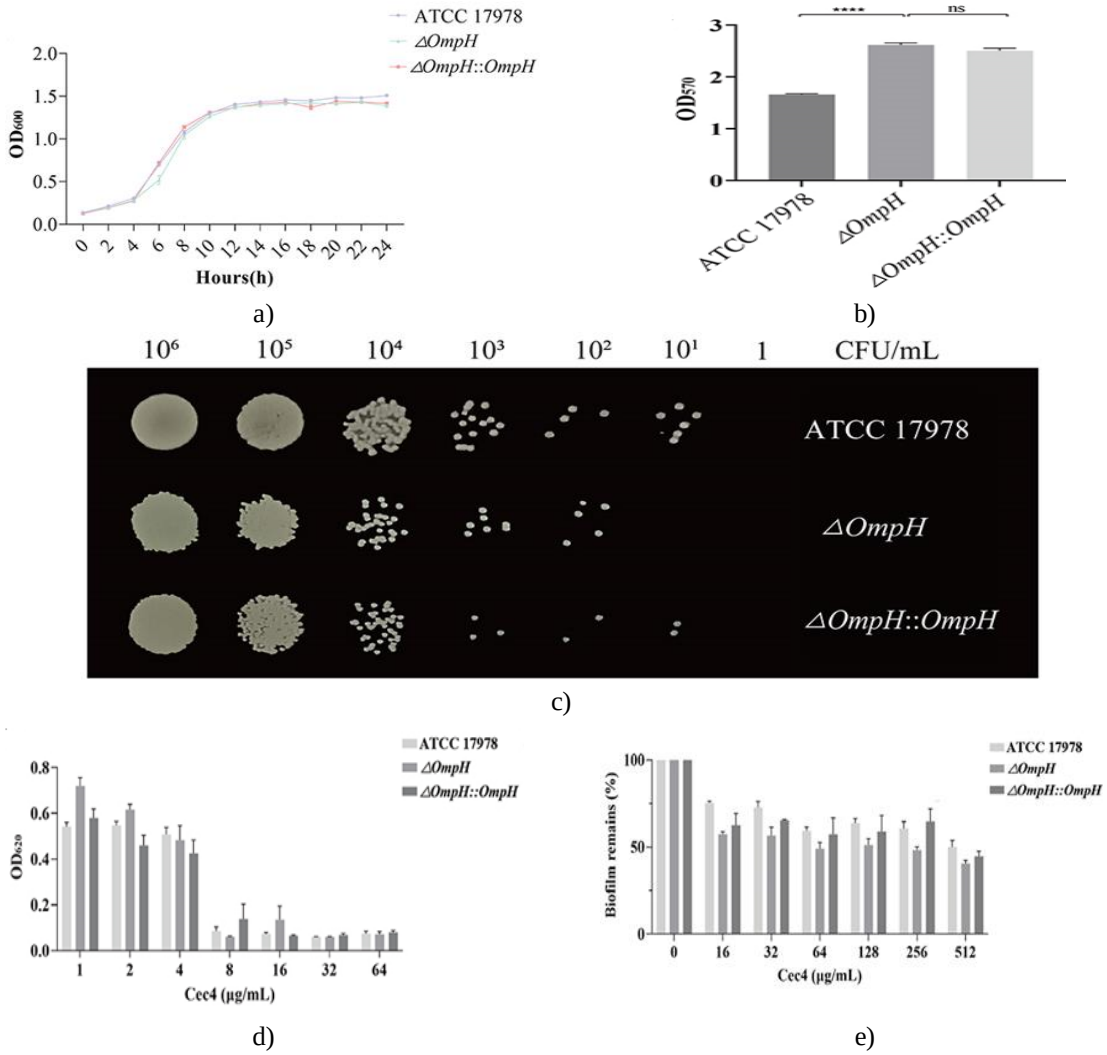

Figure 5. The impact of OmpH deletion on growth, biofilm formation, and Cec4 susceptibility. (a) Growth curves of wild-type (ATCC 17978), OmpH knockout (ΔOmpH), and back-complemented (ΔOmpH::OmpH) strains. (b) Biofilm formation and its effect on growth and susceptibility in the same strains. (c) Cec4 sensitivity of OmpH deletion strains assessed by agar spot plate. (d) OD620 measurements for MBC determination. (e) MBEC50 of antimicrobial peptide Cec4 against ATCC 17978, ΔOmpH, and ΔOmpH::OmpH.

Effect of OmpH deletion on A. baumannii sensitivity to Cec4

We assessed Cec4 susceptibility in A. baumannii following OmpH deletion. The MIC of ΔOmpH was about one dilution lower than that of ATCC 17978 (~2–4 μg/mL vs. ~4 μg/mL). Agar spot plate assays confirmed these results **(Figure 5c)**, indicating that OmpH deletion increased ATCC 17978's sensitivity to Cec4. The MBC of ΔOmpH was identical to ATCC 17978 at 8 μg/mL; although ΔOmpH biofilms were slightly thicker at 1, 2, and 16 μg/mL, differences were not statistically significant **(Figure 5d)**. MBEC50 testing revealed that Cec4 cleared ΔOmpH biofilms at 256 μg/mL, whereas ATCC 17978 did not reach 50% removal at 512 μg/mL, and ΔOmpH::OmpH reached 50% removal at 512 μg/mL. These findings suggest that ΔOmpH biofilms are slightly but significantly more susceptible to Cec4 than wild-type biofilms ($P < 0.05$) **(Figure 5e)**, implying potential interactions between OmpH and Cec4 during biofilm clearance.

Effect of OmpH on capsule thickness in A. baumannii

Capsules contribute critically to biofilm formation. Staining revealed that the extracellular region appears pink, cells purple, and the transparent layer represents the capsule. ΔOmpH strains exhibited markedly thinner capsules compared with ATCC 17978, indicating that OmpH positively influences capsule formation.

Regulatory role of OmpH in A. baumannii

We examined expression levels of biofilm-associated genes after OmpH knockout. In ΔOmpH, BfmR (part of the two-component system) was upregulated, whereas BfmS, CsuE (pili system), and phosphoglucose-mutase (PGM) were downregulated. Prior studies indicate that BfmS is negatively regulated by BfmR [34], consistent with these findings. qPCR confirmed that OmpH expression was higher in overexpressed strains, supporting its regulatory role. Coupled with reduced capsule thickness in ΔOmpH, these results suggest that the OmpH-BfmR-CsuE/PGM pathway modulates A. baumannii physiology.

Biofilms are microbial communities embedded in an extracellular matrix that protects them from environmental stress, composed of extracellular DNA, polysaccharides, proteins, and insoluble compounds [35]. Matrix composition may vary with growth conditions or external changes [36], although the regulatory mechanisms remain unclear. Previous studies demonstrated that Cec4 effectively inhibits A. baumannii biofilm formation [20, 21], but the molecular basis was unresolved, prompting the use of transcriptomics to identify key genes involved in Cec4-mediated biofilm clearance.

Transcriptomic analysis identified three KEGG pathways significantly enriched during Cec4 treatment: sulfur metabolism, ABC transporters, and the two-component system. Genes in the sulfur metabolism pathway were mainly involved in the uptake of extracellular sulfate, taurine, and alkane sulfonates, which can feed into prokaryotic carbon sequestration pathways, suggesting that Cec4 may impact bacterial carbon metabolism during biofilm removal. Other genes in this pathway, such as sulfide oxidoreductases, were also involved, and previous studies have shown that sulfur metabolism-related genes are generally upregulated during biofilm formation [37]. In the present analysis, 11 of 12 genes were upregulated, indicating that bacteria respond to Cec4-mediated biofilm clearance by increasing sulfur metabolism. Because elemental sulfur is essential for methionine and cysteine biosynthesis, Cec4 treatment may also inhibit these processes in bacteria.

The two-component system pathway was enriched with four genes related to acidic amino acid uptake and metabolism, including glnQ, gltK, HMPREF0010_00886, and gltI, which are homologs of AatP/M/Q/J genes, and these were significantly downregulated. Acidic amino acids such as aspartic and glutamic acid are reported to enhance the solubility of many insoluble drugs [38]. Additionally, genes homologous to the LuxI/LuxR quorum-sensing system, bpsI (LuxI family acyl-homoserine lactone synthase SolI) and HMPREF0010_03224 (LuxR-family regulator SolR), were upregulated in response to Cec4 in mature biofilms. Although the precise relationship between LuxI/LuxR expression and biofilm formation is unclear [39], their upregulation indicates that Cec4 influences population-sensing pathways.

KEGG enrichment also highlighted the ABC transporter pathway, with 16 co-enriched genes identified, including members of the Glt and Ssu families. Glt genes are associated with aspartic acid transport, which, when elevated, can inhibit biofilm formation and promote planktonic growth [40, 41]; their downregulation after Cec4 treatment may reflect bacterial attempts to maintain biofilm integrity. Ssu family genes, involved in aliphatic sulfonate transport, currently have no clear link to biofilm formation [42]. Notably, the efflux pump gene MacB was upregulated in Cec4-treated planktonic and biofilm A. baumannii, as well as in Cec4-induced drug-resistant strains, consistent with its role in macrolide resistance by affecting ribosomal protein function and bacterial protein

synthesis [43, 44]. This suggests that MacB upregulation may be a bacterial response to Cec4 entering cells and impacting ribosome-related processes.

Annotation of the transcriptome revealed several outer membrane-associated genes. Given that previous studies demonstrated Cec4 co-localizes with A. baumannii biofilms, outer membrane differential genes were prioritized, and OmpH was selected for knockout experiments due to its reported potential as an OmpH-like antigen. OmpH is predicted to encode a structural domain similar to OmpH proteins, which function as Skp periplasmic chaperones in E. coli. OmpH-like proteins, such as those in Flavobacterium psychrophilum, are approximately 166 amino acids with an N-terminal signal peptide, and may serve as vaccine antigens [25]. A. baumannii OmpH contains 167 amino acids with a 22-residue N-terminal signal peptide, also suggesting antigenic potential. OmpH deletion did not affect bacterial growth but enhanced biofilm formation, implying that OmpH negatively regulates biofilm production. Cec4 targeting OmpH may reinforce its inhibitory effect on biofilm formation.

Literature review indicates that BfmS, CsuE, and Pgm are negatively correlated with biofilm formation, whereas BfmR is positively correlated. RT-qPCR results showed that OmpH positively regulates BfmS, CsuE [45], and Pgm, and negatively regulates BfmR. OmpH deletion led to BfmS downregulation and BfmR upregulation. BfmR subsequently activates TetR-family transcriptional regulators [46], further repressing Pgm, reducing capsule thickness, and increasing biofilm in OmpH deletion strains. CsuE showed a slight downward trend, suggesting that OmpH primarily influences Cec4-mediated biofilm clearance rather than direct biofilm synthesis. MIC and MBEC50 values for Cec4 decreased in OmpH deletion strains, demonstrating that OmpH directly affects A. baumannii sensitivity to Cec4 and likely interacts with it, consistent with findings by Martinez-Guitian *et al.*, where OmpH deletion increased strain susceptibility [47].

Conclusion

Transcriptomic analysis identified the outer membrane protein OmpH as a key target in Cec4-mediated reduction of A. baumannii biofilms. While OmpH deletion did not alter bacterial growth, it resulted in increased biofilm formation and reduced MIC and MBEC50 values for Cec4. These findings suggest that OmpH may serve as a critical mediator in Cec4-driven biofilm clearance, representing a potential target for antimicrobial strategies against biofilm-forming A. baumannii **(Figure 6).**

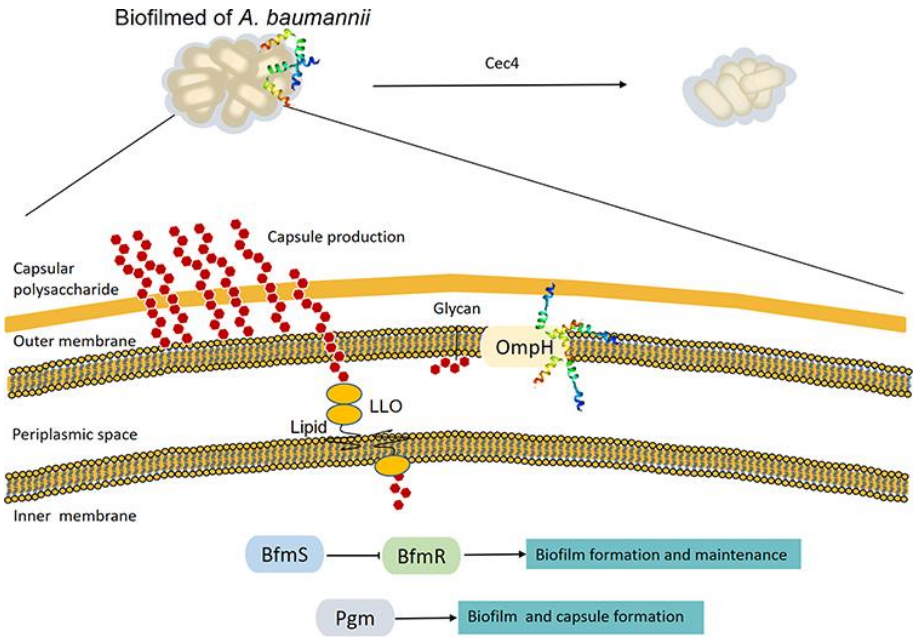

Figure 6. Cec4 reduces A. baumannii biofilms via OmpH. Deletion of the OmpH gene alters the two-component system BfmRS and Pgm, resulting in increased biofilm formation and heightened sensitivity of the knockout strain to Cec4. Glycan synthesis is initiated by a specific glycosyltransferase, which generates lipo-oligosaccharides (LLO) through the transfer of sugars to phosphorylated lipids.

Acknowledgments: None

Conflict of Interest: None

Financial Support: None

Ethics Statement: None

References

1. Peleg AY, Seifert H, Paterson DL. Acinetobacter baumannii: emergence of a successful pathogen. Clin Microbiol Rev. 2008;21(3):538–82. doi:10.1128/CMR.00058-07
2. Giammanco A, Calà C, Fasciana T, Dowzicky MJ. Global assessment of the activity of tigecycline against multidrug-resistant gram-negative pathogens between 2004 and 2014 as part of the tigecycline evaluation and surveillance trial. mSphere. 2017;2(1). doi:10.1128/mSphere.00310-16
3. Theuretzbacher U, Bush K, Harbarth S, Paul M, Rex JH, Tacconelli E, et al. Critical analysis of antibacterial agents in clinical development. Nat Rev Microbiol. 2020 May;18(5):286-98. doi:10.1038/s41579-020-0340-0
4. MacNair CR, Brown ED. Outer membrane disruption overcomes intrinsic, acquired, and spontaneous antibiotic resistance. mBio. 2020;11(5). doi:10.1128/mBio.01615-20
5. Muhammad MH, Idris AL, Fan X, Guo Y, Yu Y, Jin X, et al. Beyond Risk: Bacterial Biofilms and Their Regulating Approaches. Front Microbiol. 2020;11:928. doi:10.3389/fmicb.2020.00928
6. Upmanyu K, Haq QMR, Singh R. Factors mediating Acinetobacter baumannii biofilm formation: opportunities for developing therapeutics. Curr Res Microb Sci. 2022;3:100131. doi:10.1016/j.crmicr.2022.100131
7. Wannigama DL, Hurst C, Pearson L, Saethang T, Singkham-In U, Luk-In S, et al. Simple fluorometric-based assay of antibiotic effectiveness for Acinetobacter baumannii biofilms. Sci Rep. 2019;9(1):6300. doi:10.1038/s41598-019-42353-0
8. Shenkutie AM, Zhang J, Yao M, Asrat D, Chow FWN, Leung PHM. Effects of sub-minimum inhibitory concentrations of imipenem and colistin on expression of biofilm-specific antibiotic resistance and virulence genes in Acinetobacter baumannii sequence type 1894. Int J Mol Sci. 2022;23(20):12705. doi:10.3390/ijms232012705
9. Lebeaux D, Ghigo JM, Beloin C. Biofilm-related infections: bridging the gap between clinical management and fundamental aspects of recalcitrance toward antibiotics. Microbiol Mol Biol Rev. 2014;78(3):510–43. doi:10.1128/MMBR.00013-14
10. Sun F, Qu F, Ling Y, Mao P, Xia P, Chen H, et al. Biofilm-associated infections: antibiotic resistance and novel therapeutic strategies. Future Microbiol. 2013;8(7):877-86. doi:10.2217/fmb.13.58
11. Chung PY, Khanum R. Antimicrobial peptides as potential anti-biofilm agents against multidrug-resistant bacteria. J Microbiol Immunol Infect. 2017;50(4):405–10. doi:10.1016/j.jmii.2016.12.005
12. Bahar AA, Ren D. Antimicrobial peptides. Pharmaceuticals. 2013;6(12):1543–75. doi:10.3390/ph6121543
13. Saikia K, Sravani YD, Ramakrishnan V, Chaudhary N. Highly potent antimicrobial peptides from N-terminal membrane-binding region of E. coli MreB. Sci Rep. 2017;7:42994. doi:10.1038/srep42994
14. Luo Y, Song Y. Mechanism of antimicrobial peptides: antimicrobial, anti-inflammatory and antibiofilm activities. Int J Mol Sci. 2021;22(21):11401. doi:10.3390/ijms222111401
15. Overhage J, Campisano A, Bains M, Torfs EC, Rehm BH, Hancock RE. Human host defense peptide LL-37 prevents bacterial biofilm formation. Infect Immun. 2008;76(9):4176–82. doi:10.1128/IAI.00318-08
16. Wolz C, Geiger T, Goerke C. The synthesis and function of the alarmone (p)ppGpp in firmicutes. Int J Med Microbiol. 2010;300(2–3):142–7. doi:10.1016/j.ijmm.2009.08.017
17. Di Somma A, Moretta A, Canè C, Cirillo A, Duilio A. Antimicrobial and antibiofilm peptides. Biomolecules. 2020;10(4):652. doi:10.3390/biom10040652
18. Naclerio GA, Sintim HO. Multiple ways to kill bacteria via inhibiting novel cell wall or membrane targets. Future Med Chem. 2020;12(13):1253–79. doi:10.4155/fmc-2020-0046

19. Peng J, Long H, Liu W, Wu Z, Wang T, Zeng Z, et al. Antibacterial mechanism of peptide Cec4 against Acinetobacter baumannii. Infect Drug Resist. 2019;12:2417-28. doi:10.2147/IDR.S214057
20. Peng J, Wang Y, Wu Z, Mao C, Li L, Cao H, et al. Antimicrobial peptide Cec4 eradicates multidrug-resistant Acinetobacter baumannii in vitro and in vivo. Drug Des Devel Ther. 2023;17:977-92. doi:10.2147/DDDT.S405579
21. Liu W, Wu Z, Mao C, Guo G, Zeng Z, Fei Y, et al. Antimicrobial peptide Cec4 eradicates the bacteria of clinical carbapenem-resistant Acinetobacter baumannii biofilm. Front Microbiol. 2020;11:1532. doi:10.3389/fmicb.2020.01532
22. Jumper J, Evans R, Pritzel A, Green T, Figurnov M, Ronneberger O, et al. Highly accurate protein structure prediction with alphafold. Nature. 2021;596(7873):583-9. doi:10.1038/s41586-021-03819-2. Epub 2021 Jul 15. PMID: 34265844; PMCID: PMC8371605.
23. Chen N, Jiang D, Liu Y, Zhang Z, Zhou Y, Zhu Z. Preparation of Escherichia coli ghost of anchoring bovine Pasteurella multocida OmpH and its immunoprotective effect. BMC Vet Res. 2023;19(1):192. doi:10.1186/s12917-023-03743-9
24. Saier MH, Ma CH, Rodgers L, Tamang DG, Yen MR. Protein secretion and membrane insertion systems in bacteria and eukaryotic organelles. Adv Appl Microbiol. 2008;65:141–97. doi:10.1016/j.aam.2008.01.001
25. Dumetz F, Duchaud E, LaPatra SE, Le Marrec C, Claverol S, Urdaci MC, et al. A protective immune response is generated in rainbow trout by an OmpH-like surface antigen (P18) of flavobacterium psychrophilum. Appl Environ Microbiol. 2006;72(7):4845-52. doi:10.1128/AEM.00279-06
26. Jia J, Zhao M, Ma K, Zhang H, Gui L, Sun H, et al. The immunoprotection of *OmpH* gene deletion mutation of *pasteurella multocida* on hemorrhagic sepsis in qinghai yak. Vet Sci. 2023;10(3):221. doi:10.3390/vetsci10030221. PMID: 36977260; PMCID: PMC10055848.
27. Lahesmaa R, Skurnik M, Vaara M, Leirisalo-Repo M, Nissilä M, Granfors K, et al. Molecular mimickry between HLA B27 and Yersinia, Salmonella, Shigella and Klebsiella within the same region of HLA alpha 1-helix. Clin Exp Immunol. 1991;86(3):399-404. doi:10.1111/j.1365-2249.1991.tb02944.x. PMID: 1747948; PMCID: PMC1554211.
28. Wang Y, Wang Z, Chen Y, Hua X, Yu Y, Ji Q. A highly efficient CRISPR-Cas9-based genome engineering platform in Acinetobacter baumannii to understand the H(2)O(2)-sensing mechanism of OxyR. Cell Chem Biol. 2019;26(12):1732–42.e1735. doi:10.1016/j.chembiol.2019.09.003
29. O'Toole GA. Microtiter dish biofilm formation assay. J Vis Exp. 2011;(47):2437. doi:10.3791/2437. PMID: 21307833; PMCID: PMC3182663.
30. Wiegand I, Hilpert K, Hancock RE. Agar and broth dilution methods to determine the minimal inhibitory concentration (MIC) of antimicrobial substances. Nat Protoc. 2008;3(2):163–75. doi:10.1038/nprot.2007.521
31. Pedonese F, Longo E, Torracca B, Najar B, Fratini F, Nuvoloni R. Antimicrobial and anti-biofilm activity of manuka essential oil against Listeria monocytogenes and Staphylococcus aureus of food origin. Italian J Food Safety. 2022;11(1):10039. doi:10.4081/ijfs.2022.10039
32. Abouelhassan Y, Yang Q, Yousaf H, Nguyen MT, Rolfe M, Schultz GS, et al. Nitroxoline: a broad-spectrum biofilm-eradicating agent against pathogenic bacteria. Int J Antimicrob Agents. 2017;49(2):247-51. doi:10.1016/j.ijantimicag.2016.10.017. Epub 2016 Dec 6. PMID: 28110918.
33. Zhang Y, Wu X, Cai J, Chen M, Zhang J, Shao S, et al. Transposon insertion sequencing analysis unveils novel genes involved in luxR expression and quorum sensing regulation in Vibrio alginolyticus. Microbiol Res. 2023;267:127243. doi:10.1016/j.micres.2022.127243. Epub 2022 Nov 11. PMID: 36521340.
34. Krasauskas R, Skerniškytė J, Armalytė J, Sužiedėlienė E. The role of Acinetobacter baumannii response regulator BfmR in pellicle formation and competitiveness via contact-dependent inhibition system. BMC Microbiol. 2019;19(1):241. doi:10.1186/s12866-019-1621-5
35. Neu TR, Lawrence JR. In situ characterization of Extracellular Polymeric Substances (EPS) in biofilm systems. In: Wingender J, Neu TR, Flemming H-C, editors. Microbial Extracellular Polymeric Substances: Characterization, Structure and Function. Berlin, Heidelberg: Springer Berlin Heidelberg; 1999:21–47. doi:10.1007/978-3-642-60147-7
36. Flemming HC, van Hullebusch ED, Neu TR, Nielsen PH, Seviour T, Stoodley P, et al. The biofilm matrix: multitasking in a shared space. Nat Rev Microbiol. 2023;21(2):70-86. doi:10.1038/s41579-022-00791-0. Epub 2022 Sep 20. PMID: 36127518.

37. Zhang W, Wu Y, Wu J, Zheng X, Chen Y. Enhanced removal of sulfur-containing organic pollutants from actual wastewater by biofilm reactor: insights of sulfur transformation and bacterial metabolic traits. Environ Pollut. 2022;313:120187. doi:10.1016/j.envpol.2022.120187
38. Warraich AA, Mohammed AR, Perrie Y, Hussain M, Gibson H, Rahman A. Evaluation of anti-biofilm activity of acidic amino acids and synergy with ciprofloxacin on Staphylococcus aureus biofilms. Sci Rep. 2020;10(1):9021. doi:10.1038/s41598-020-66082-x
39. Li Y, Wang B, Lu F, Ahn J, Zhang W, Cai L, et al. Synergistic inhibitory effect of polymyxin B in combination with ceftazidime against robust biofilm formed by Acinetobacter baumannii with genetic deficiency in AbaI/AbaR quorum sensing. Microbiol Spectr. 2022;10(1): 0176821. doi:10.1128/spectrum.01768-21. Epub 2022 Feb 23. PMID: 35196792; PMCID: PMC8865539.
40. McIlwain BC, Vandenberg RJ, Ryan RM. Characterization of the inward- and outward-facing substrate binding sites of the prokaryotic aspartate transporter, Glt(Ph). Biochemistry. 2016;55(49):6801–10. doi:10.1021/acs.biochem.6b00795
41. Su X, Cheng X, Wang Y, Luo J. Effect of different D-amino acids on biofilm formation of mixed microorganisms. Wat Sci Technol. 2022;85(1):116–24. doi:10.2166/wst.2021.623
42. Beale J, Lee SY, Iwata S, Beis K. Structure of the aliphatic sulfonate-binding protein SsuA from Escherichia coli. Acta Crystallogr F. 2010;66(4):391–6. doi:10.1107/S1744309110006226
43. Greene NP, Kaplan E, Crow A, Koronakis V. Antibiotic resistance mediated by the MacB ABC transporter family: a structural and functional perspective. Front Microbiol. 2018;9:950. doi:10.3389/fmicb.2018.00950
44. Dinos GP. The macrolide antibiotic renaissance. Br J Pharmacol. 2017;174(18):2967–83. doi:10.1111/bph.13936
45. De Breij A, Gaddy J, van der Meer J, Koning R, Koster A, van den Broek P, et al. CsuA/BABCDE-dependent pili are not involved in the adherence of Acinetobacter baumannii ATCC19606(T) to human airway epithelial cells and their inflammatory response. Res Microbiol. 2009;160(3):213-8. doi:10.1016/j.resmic.2009.01.002. PMID: 19530313.
46. Fidopiastis PM, Miyamoto CM, Jobling MG, Meighen EA, Ruby EG. LitR, a new transcriptional activator in Vibrio fischeri, regulates luminescence and symbiotic light organ colonization. Mol Microbiol. 2002;45(1):131–43. doi:10.1046/j.1365-2958.2002.02996.x
47. Birkle K, Renschler F, Angelov A, Wilharm G, Franz-Wachtel M, Maček B, et al. An unprecedented tolerance to deletion of the periplasmic chaperones sura, skp, and degp in the nosocomial pathogen Acinetobacter baumannii. J Bacteriol. 2022;204(10): 0005422. doi:10.1128/jb.00054-22. Epub 2022 Sep 15. PMID: 36106853; PMCID: PMC9578438.